E1-2003-67

L. V. Chkhaidze[1], T. D. Djobava[1], V. R. Garsevanishvili[2],
L. L. Kharkhelauri[1], E. N. Kladnitskaya, A. A. Kuznetsov,
G. O. Kuratashvili[1]

THE ANALYSIS OF π^--MESON SPECTRA IN SEMICENTRAL CC AND CTa COLLISIONS AT A MOMENTUM OF 4.2 GeV/c PER NUCLEON IN TERMS OF LIGHT FRONT VARIABLES

Submitted to «Ядерная физика»

[1]High Energy Physics Institute, Tbilisi State University, Georgia
E-mail: ida@sun20.hepi.edu.ge or ichkhaidze@yahoo.com
[2]Mathematical Institute of the Georgian Academy of Sciences, Georgia

1. INTRODUCTION

The study of single particle inclusive processes [1] remains one of the simplest and effective tools for the investigation of multiple production of secondaries at high energies. The consequences of the limiting fragmentation hypothesis [2] and those of the parton model [3] and the principle of automodelity for strong interactions [4] have been formulated in this way.

At high energies, different dynamical mechanisms contribute to the spectra of secondaries. Among them, "pionization" and fragmentation mechanisms have been widely discussed. "Pionization" means the existence of secondary pions with relatively low momenta and a flat (almost isotropic) angular distribution in the center-of-mass frame of colliding objects. The fragmentation component has a sharply anisotropic angular distribution in the center-of-mass frame. One of the principal problems in this direction is the separation of these two components. Up to now, there exits no unique way to separate these mechanisms. Different authors propose different ways and none of them seems to be satisfactory. It will be shown that the presentation of inclusive spectra in terms of light front variables provides a unique possibility to separate these two components.

An important role in establishing the properties of multiple particle production plays the choice of kinematic variables in terms of which the observable quantities are presented (see e.g. [5,6,7]).

In this paper, we continue the study of π mesons produced in relativistic nucleus–nucleus collisions in terms of light front variables. The choice of light front variables is due to the fact that these variables seem to be more sensitive to the interaction dynamics as compared to the well-known Feynman variables x_F and rapidity y.

The light front analysis of π^- mesons produced in He(Li,C), CNe, CCu, CPb and MgMg collisions at a momentum of 4.5 GeV/c per nucleon has been performed in the previous publications [8,9]. The data were obtained on the SKM-200-GIBS facility of the Joint Institute for Nuclear Research in Dubna. On the basis of this analysis, we were able to separate the phase space region, where thermal equilibrium seems to be achieved. The same analysis was performed on a part of inelastic CC and CTa collisions at a momentum of 4.2 GeV/c per nucleon registered in the 2 meter Propane Bubble Chamber of JINR [10]. In this paper, the spectra of pions from semicentral CC and CTa collisions at a momentum of 4.2 GeV/c per nucleon are studied in terms of light front variables. Semicentral collisions were separated from the whole ensemble of inelastic CC and CTa interactions identified unambiguously.

2. EXPERIMENT

The data were obtained on the 2 m Propane Bubble Chamber of JINR. The chamber was placed in a magnetic field of 1.5 T. Three Ta plates (140x70x1) mm^3 in size mounted into the fiducial volume of the chamber at a distance of 93 mm from each other served as a nuclear target. The separation method of CC collisions in propane, data processing, identification of particles and discussion of corrections are described in detail in [11]. Apart from the unambiguously identified CC collisions with the ωe probability equal one, the experimental data contain also the sample of CC events with $\omega e = 0.21$. When studying the inclusive characteristics of CC collisions, the distributions are obtained for the whole ensemble of CC collisions taking into account the weight factor ωe.

The sub-sample of "semicentral" events with the number of participant protons $N_{\rm part} \geq 4$ were selected for the analysis from the whole ensemble of CC and CTa collisions. With this aim, the target fragments ($p < 0.3$ GeV/c for CC and $p < 0.2$ GeV/c for CTa), projectile stripping ($p > 3$ GeV/c and angle $\theta < 4^o$) fragments and also light projectile fragments with $Z > 1$ (^{3}He,^{4}He) identified by ionization visually and π mesons were excluded from the whole ensemble of secondary particles.

An additional identification of π^+ mesons was performed [12] in order to separate participant protons since π^+ mesons were identified in a narrow interval of momenta up to 0.5 GeV/c in the propane chamber. For the particles with $p > 0.5$ GeV/c in all CC collisions special statistical weights were introduced for π^+ meson and proton hypothesis separately. The separation of the group of CC collisions with $\omega e = 1$ and the necessity of unambiguous separation of protons and π^+ mesons led to the difference in the momentum distributions of π^- and π^+ mesons. To remove this difference, the correction of π^+ meson identification was made. The procedure was performed for CC and CTa events statistically with the assumption that the distributions of π^- and π^+ mesons must be similar.

In consequence, the group of semicentral 9500 (20477 π^- mesons) CC and 1620 CTa (11318 $\pi^\pm$ mesons) collisions was separated from inelastic 15965 CC (25409 π^- mesons) and 2469 CTa (12160 $\pi^\pm$ mesons) collisions.

3. LIGHT FRONT PRESENTATION OF INCLUSIVE DISTRIBUTIONS

Here, we propose unified scale invariant variables for the presentation of single particle inclusive distributions, the properties of which are described below.

Consider an arbitrary 4–momentum $p_\mu(p_0, \vec{p})$ and introduce light front combinations [13]:

$$p_\pm = p_0 \pm p_3. \tag{1}$$

If the 4–momentum p_μ is on the mass shell ($p^2 = m^2$), the combinations $p_\pm$, $\vec{p}_T$ (where $\vec{p}_T = (p_1,\ p_2)$) define the so-called horospherical coordinate system (see, e.g. [14]) on the corresponding mass shell hyperboloid $p_0^2 - \vec{p}^{\,2} = m^2$.

Let us construct the scale invariant variables [15]:

$$\xi^\pm = \pm \frac{p_\pm^c}{p_\pm^a + p_\pm^b} \tag{2}$$

in terms of the 4–momenta p_μ^a, p_μ^b, p_μ^c of particles a, b, c, entering from the inclusive reaction $a + b \to c + X$. The z-axis is taken to be the collision axis, i.e. $p_z = p_3 = p_L$. Particles a and b can be hadrons, heavy ions, leptons. The light front variables $\xi^\pm$ in the center-of-mass frame are defined as follows [15]:

$$\xi^\pm \ = \ \pm \frac{E \pm p_z}{\sqrt{s}} = \pm \frac{E + |p_z|}{\sqrt{s}} \tag{3}$$

where s is the usual Mandelstam variable, $E = \sqrt{p_z^2 + p_T^2 + m^2}$ and p_z are the energy and the z - component of the momentum of produced particle. The upper sign in Eq. (3) is used for the right-hand side hemisphere and the lower sign for the left-hand side one. It is also convenient to introduce the variables

$$\zeta^\pm = \mp \ln|\xi^\pm| \tag{4}$$

in order to enlarge the scale in the region of small $\xi^\pm$. The invariant differential cross section in terms of these variables looks as follows:

$$E\frac{d\sigma}{d\vec{p}} = \frac{|\xi^\pm|}{\pi} \frac{d\sigma}{d\xi^\pm dp_T^2} = \frac{1}{\pi} \frac{d\sigma}{d\zeta^\pm dp_T^2}\ . \tag{5}$$

In the limits of high p_z ($|p_z| \gg p_T$) and high p_T ($p_T \gg |p_z|$), the $\xi^\pm$ variables go over to the well-known variables $x_F = 2p_z/\sqrt{s}$ and $x_T = 2p_T/\sqrt{s}$, respectively, which are intensively used in high energy physics. The $\xi^\pm$–variables are related to x_F, x_T and rapidity y as follows:

$$\xi^\pm \ = \ \frac{1}{2}\left(x_F \pm \sqrt{x_F^2 + x_T^2}\right) \ ; \ x_T = \frac{2m_T}{\sqrt{s}} \tag{6}$$

$$y \ = \ \pm\frac{1}{2} \ln \frac{(\xi^\pm\sqrt{s})^2}{m_T^2} \ ; \ m_T = \sqrt{p_T^2 + m^2}\ . \tag{7}$$

This variables are widely used in the treatment of many theoretical problems (see, e.g. original and review papers [16-21]).

4. THE ANALYSIS OF PION DISTRIBUTIONS IN TERMS OF LIGHT FRONT VARIABLES

The analysis in CC collisions has been carried out for the π^- mesons. To increase small statistics of CTa collisions, the data on π^- and π^+ mesons have been combined. Figure 1 presents the $\xi^{\pm}$ – distributions of π^- mesons in CC and π^- and π^+ mesons in CTa interactions. The principal differences of the $\xi^{\pm}$ distributions and x_F – distributions (Fig. 2) are the following: (1) the existence of a forbidden region around the point $\xi^{\pm} = 0$; (2) the existence of maxima at some $\tilde{\xi^{\pm}}$ in the region of relatively small $|\xi^{\pm}|$; (3) the existence of the limits for $|\xi^{\pm}| \leq m/\sqrt{s}$.

The experimental data for the invariant distributions $(1/\pi) \cdot dN/d\zeta^{\pm}$ are shown in Fig. 3. As the ξ and ζ distributions for CC collisions are symmetric, the data have been analyzed over the whole range ($\xi^{\pm}$, $\zeta^{\pm}$) of the ξ and ζ variables. The CTa data have been analyzed only in the forward hemisphere (ξ^{+}, ζ^{+}). The maxima at $\tilde{\zeta^{\pm}}$ are also observed in the invariant distributions $(1/\pi) \cdot dN/d\zeta^{\pm}$. However, the region $|\xi^{\pm}| > |\tilde{\xi^{\pm}}|$ goes over to the region $|\zeta^{\pm}| < |\tilde{\zeta^{\pm}}|$ and vice versa (see Eqs. (3) and (4)). Maxima are observed at $\tilde{\zeta^{\pm}} = 1.95 \pm 0.05$ for CC and $\tilde{\zeta^{\pm}} = 2.00 \pm 0.05$ for CTa. The $\tilde{\zeta^{\pm}}$ is the function of energy (see Eqs. (3), (4)) and does not depend on the projectile (A_P) and target (A_T) masses.

In order to study the nature of these maxima we have divided the phase space into two regions $|\zeta^{\pm}| > |\tilde{\zeta^{\pm}}|$ and $|\zeta^{\pm}| < |\tilde{\zeta^{\pm}}|$ and studied the p_T^2 and angular distributions of π mesons in these regions separately. For example, the number of pions in CTa interactions in the region $\zeta^{+} > \tilde{\zeta}^{+}$ is equal to – 2770 and 3904 in $\zeta^{+} < \tilde{\zeta}^{+}$. The angular and p_T^2 distributions of π mesons from CC and CTa interactions in different regions of $\zeta^{\pm}$ are presented in Figs. 4 and 5.

From Figs. 4 and 5, one can see that the angular and p_T^2 distributions of pions in CC and CTa differ significantly in the $|\zeta^{\pm}| > |\tilde{\zeta^{\pm}}|$ and $|\zeta^{\pm}| < |\tilde{\zeta^{\pm}}|$ regions. The angular distribution of pions in the region $|\zeta^{\pm}| < |\tilde{\zeta^{\pm}}|$ (Figs. 4.a and 4.b) is sharply anisotropic in contrast to an almost flat distribution in the region $|\zeta^{\pm}| > |\tilde{\zeta^{\pm}}|$ (Figs. 4.a and 4.b). A flat behavior of the angular distribution allows one to think that a partial thermal equilibrium is observed in the region $|\zeta^{\pm}| > |\tilde{\zeta^{\pm}}|$ ($|\xi^{\pm}| < |\tilde{\xi^{\pm}}|$) of phase space. The slopes of the p_T^2

– distributions differ greatly in different regions of $\zeta^{\pm}$ (Figs. 5.a and 5.b). Thus, the values of $\tilde{\zeta^{\pm}}$ are the boundaries of two regions with significantly different characteristics of pions. The validity of this statement can be seen from the momentum distributions of π^- mesons in the laboratory frame. Figure 6 presents the momentum distribution of pions from CC (Fig 6.a) and CTa (Fig 6.b) collisions in the laboratory frame. The shaded area corresponds to the region – $\zeta^+ > \tilde{\zeta^+}$ and the non-shaded one to the region – $0 < \zeta^+ < \tilde{\zeta^+}$. As can be seen from Fig. 6, these two regions almost do not overlap in the momentum space. Pions from the region– $\zeta^+ > \tilde{\zeta^+}$ have a small momentum, up to 0.5 GeV/c. The pions from $\zeta^+ < \tilde{\zeta^+}$ region have the momentum from $\sim$ 0.5 GeV/c to 3 GeV/c. Figure 7 presents the $< p >_{\rm lab}$ dependence on $\theta_{\rm lab}$ for both pairs of nuclei in the $\zeta^+ > \tilde{\zeta^+}$ and $\zeta^+ < \tilde{\zeta^+}$ regions. The shapes of these dependencies are different. It is necessary to say, that with the increasing of A_P, A_T – $< p >_{\rm lab}$ decreases and $< \theta >_{\rm lab}$ increases.

To describe the spectra in the region – $\zeta^{\pm} > \tilde{\zeta^{\pm}}$, the Boltzmann $f(E) \sim e^{-E/T}$ – distribution has been used.

The $1/\pi \cdot dN/d\zeta^{\pm}$, dN/dp_T^2, $dN/dcos\theta$ distributions in this region look as follows :

$$\frac{1}{\pi}\frac{dN}{d\zeta^{\pm}} \sim \int_0^{p_{T,max}^2} Ef(E)dp_T^2 \tag{8}$$

$$\frac{dN}{dp_T^2} \sim \int_0^{p_{z,max}} f(E)dp_z \tag{9}$$

$$\frac{dN}{d\cos\theta} \sim \int_0^{p_{max}} f(E)p^2dp \tag{10}$$

$$E = \sqrt{\vec{p}^2 + m_\pi^2}\ ,\ \vec{p}^2 = p_z^2 + p_T^2 \tag{11}$$

where:

$$p_{T,max}^2 = (\tilde{\xi^{\pm}}\sqrt{s})^2 - m_\pi^2$$

$$p_{z,max} = [p_T^2 + m^2 - (\tilde{\xi^{\pm}}\sqrt{s})^2]/(-2\tilde{\xi^{\pm}}\sqrt{s})$$

$$p_{max} = (-\tilde{\xi^{\pm}}\sqrt{s}cos\theta + \sqrt{(\tilde{\xi^{\pm}}\sqrt{s})^2 - m_\pi^2 sin^2\theta})/sin^2\theta\ .$$

The experimental distributions in the region $\zeta^{\pm} > \tilde{\zeta^{\pm}}$ have been fitted by expressions (8), (9), (10), respectively. The results of the fit of the $dN/dcos\theta$, dN/dp_T^2, $1/\pi \cdot dN/d\zeta^{\pm}$ distributions are given in Table 1 and Figs. 4, 5. They show a good agreement with experiment. The values of the parameter T obtained by fitting the data with the Boltzmann distribution are presented in Table 1 .

The spectra of π^- mesons in the region $\zeta^{\pm} > \tilde{\zeta^{\pm}}$ are satisfactorily described by the formulae which follow from thermal equilibrium. The same formulae, extrapolated to the

region $\zeta^{\pm} < \tilde{\zeta^{\pm}}$, deviate significantly from the data. Therefore, in the region $\zeta^{\pm} < \tilde{\zeta^{\pm}}$, the p_T^2 – distributions have been fitted by the formula:

$$\frac{dN}{dp_T^2} \sim \alpha \cdot e^{-\beta_1 P_T^2} + (1-\alpha) \cdot e^{-\beta_2 p_T^2} \tag{12}$$

and the $\zeta^{\pm}$ – distributions by the formula:

$$\frac{1}{\pi} \cdot \frac{dN}{d\zeta^{+}} \sim (1-\xi^{+})^n = (1-e^{-|\zeta^{+}|})^n. \tag{13}$$

The latter is an analogue of the $(1-x_F)^n$ dependence – the result of the well-known quark-parton model consideration (see e.g. [22]) which gives n=3 for π^- mesons. The dependence $(1-e^{-|\zeta^{\pm}|})^n$ is in good agreement with experiment in the region $\zeta^{\pm} < \tilde{\zeta^{\pm}}$ and deviates from it in the region $\zeta^{\pm} > \tilde{\zeta^{\pm}}$. The results of the fit are given in Table 2 and Fig. 5.

Thus, in the $\zeta^{\pm}$ ($\xi^{\pm}$) distributions we have singled out points $\tilde{\zeta^{\pm}}$ ($\tilde{\xi^{\pm}}$) which separate in the phase space on two regions with significantly different characteristics. There are no such points in the x_F and y - distributions.

In this paper the Quark Gluon String Model (QGSM) [23] is used for comparison with the experimental data.

A detailed description and comparison of the QGSM with experimental data over a wide energy range can be found in [8,9,24]. The model yields a generally good overall fit to most experimental data [24,25].

We have generated CC and CTa interactions using the Monte–Carlo generator COLLI [26] based on the QGSM.

In the COLLI generator, there are two possibilities to generate events: 1) at unfixed impact parameter $\tilde{b}$ and 2) at fixed b.

At the first step, the version of the generation program with unfixed impact parameter $\tilde{b}$ has been used. 50000 CC and 10000 CTa inelastic collisions at a momentum of 4.2 GeV/c have been generated. Then similarly as for the experimental data, the selection criteria of participant protons have been applied on these events, namely the target fragments ($p < 0.3$ GeV/c for CC and $p < 0.2$ GeV/c for CTa) and the projectile strippings ($p > 3$ GeV/c and angle $\theta < 4^o$) have been excluded. From the analysis of generated events the protons with deep angles greater than 60^o have been excluded additionally, because such vertical tracks are registered with less efficiency in the experiment. After selection of events with the number of participant protons not less than 4, for the analysis remains the group of semicentral collisions. For this events from the impact parameter distribution, the mean values of $\langle b \rangle = 2.65 \pm 0.02$ fm for CC and $\langle b \rangle = 5.65 \pm 0.03$ for CTa semicentral interactions have been obtained.

Table 1. The results of fitting the distributions of pions in the region $\zeta^{\pm} > \tilde{\zeta^{\pm}}$ by Eqs. (8), (9) and (10).

Reaction	$\tilde{\zeta^{\pm}}$	Type of event	$T\ (MeV)$		
			$1/\pi \cdot dN/d\zeta^{+}$	$dN/dcos\theta$	dN/dP_T^2
$CC \to \pi^{-} + X$	1.95±0.05	Exp.	86±2	67±3	79±1
		QGSM	88±1	62±1	81±1
$CTa \to \pi^{\pm} + X$	2.00±0.05	Exp.	63±2	59±5	64±2
		QGSM	66±1	66±2	70±1

Table 2. The results of the fit of the distributions of π^- mesons in the region $\zeta^+ < \tilde{\zeta^+}$ by Eqs. (12) and (13).

Reaction	Type of event	dN/dp_T^2			$1/\pi * dN/d\zeta^+$
		α	β_1 $(GeV/c)^{-2}$	β_2 $(GeV/c)^{-2}$	n
$CC \to \pi^- + X$	Exp.	0.71 ± 0.06	16.2 ± 1.4	5.9 ± 0.5	3.4 ± 0.6
	QGSM	0.69 ± 0.03	24.0 ± 3.0	8.7 ± 0.1	4.1 ± 0.1
$CTa \to \pi^\pm + X$	Exp.	0.76 ± 0.03	24.6 ± 2.0	7.1 ± 0.4	2.8 ± 0.1
	QGSM	0.66 ± 0.10	22.5 ± 3.0	8.1 ± 0.2	2.5 ± 0.3

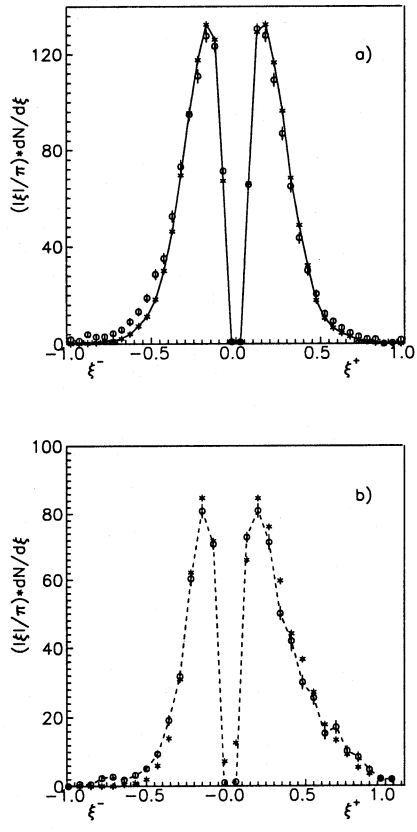

Figure 1: The $\xi^{\pm}$ – distribution of pions from a) CC collisions, b) CTa collisions : o – experimental data, $*$ – QGSM data. The curves are the result of spline approximation of the experimental data in order to guide the eye.

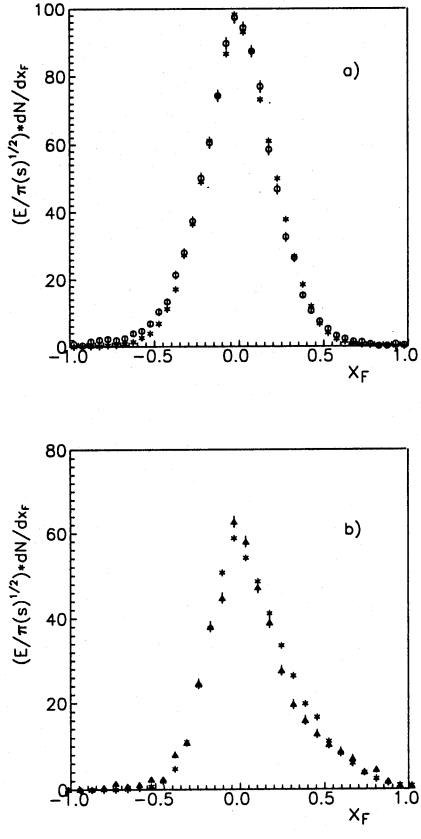

Figure 2: The x_F – distribution of pions from a) CC collisions, b) CTa collisions : $\circ$ – experimental data, $*$ – QGSM data.

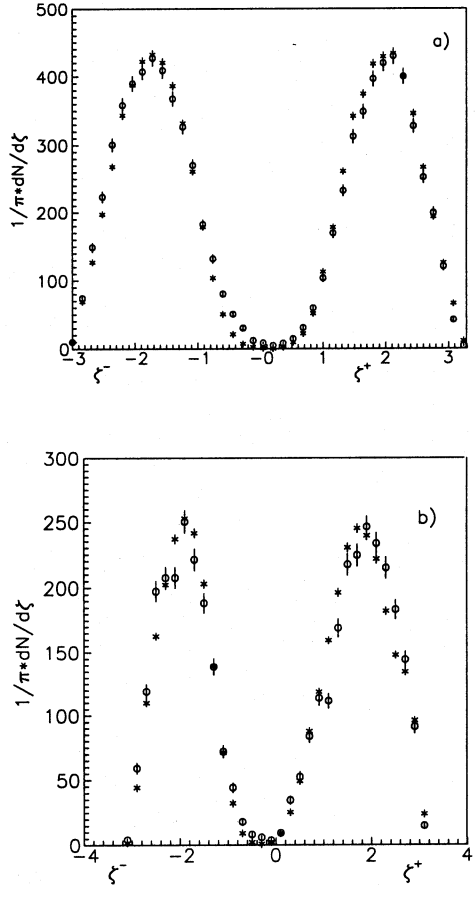

Figure 3. The $\zeta^{\pm}$ – distribution of pions from a) CC collisions, b) CTa collisions : $\circ$ – experimental data, $*$ – QGSM data.

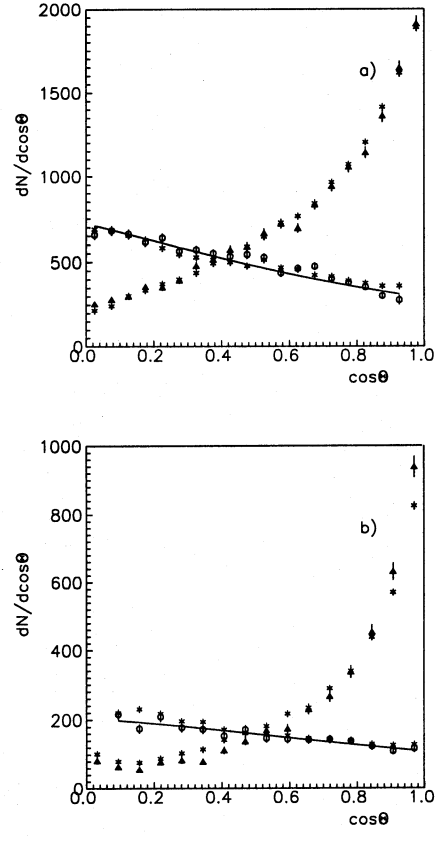

Figure 4: The $cos\theta$ distribution of pions from a) CC collisions, b) CTa collisions : $\circ$ – experimental data for $\zeta^{\pm} > \tilde{\zeta^{\pm}}$, $\triangle$ – experimental data for $\zeta^{\pm} < \tilde{\zeta^{\pm}}$, $*$ – QGSM data in both regions. The solid lines - fit of the experimental data in the region $\zeta^{\pm} > \tilde{\zeta^{\pm}}$ by Eq.(10).

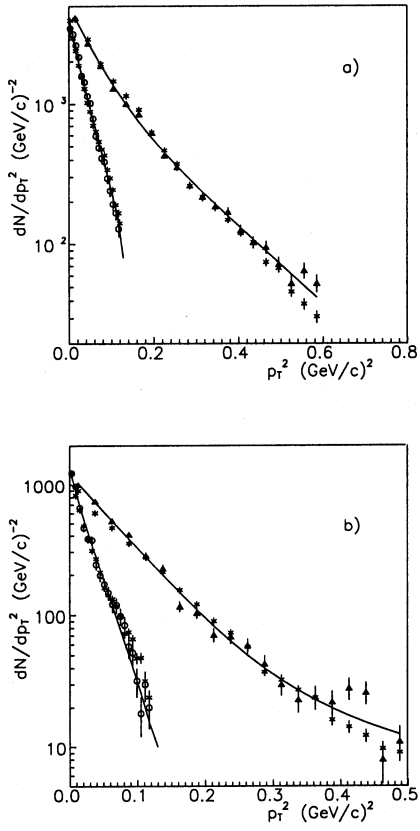

Figure 5. The p_T^2 distribution of pions from a) CC collisions, b) CTa collisions : o – experimental data for $\zeta^{\pm} > \tilde{\zeta^{\pm}}$, $\triangle$ – experimental data for $\zeta^{\pm} < \tilde{\zeta^{\pm}}$, $*$ – QGSM data in both regions. The solid lines - fit of the experimental data in the regions $\zeta^{\pm} > \tilde{\zeta^{\pm}}$ and $\zeta^{\pm} < \tilde{\zeta^{\pm}}$ by Eqs.(9) and (12), respectively.

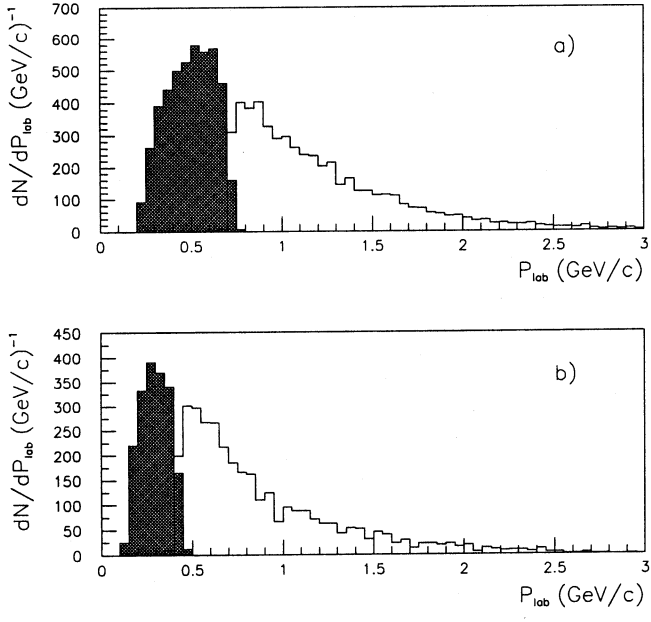

Figure 6. The momentum distribution of pions in the laboratory frame from a) CC collisions, b) CTa collisions. The shaded areas correspond to the region $\zeta^+ > \tilde{\zeta^+}$.

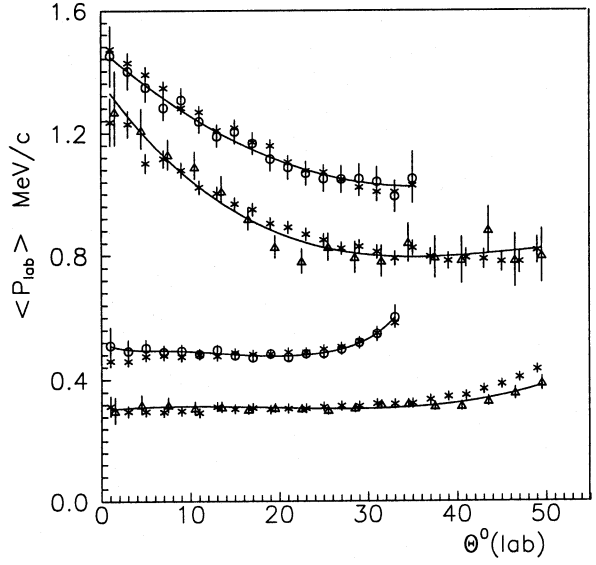

Figure 7: The $< p >_{lab}$ dependence of on Θ_{lab} in the regions $\zeta^+ > \tilde{\zeta^+}$ (bottom data) and $0 < \zeta^+ < \tilde{\zeta^+}$ (top data). $\circ$ – CC collisions, $\triangle$ – CTa collisions, $*$ – QGSM data in both regions for both pairs of nuclei. The curves – result of polynomial approximation.

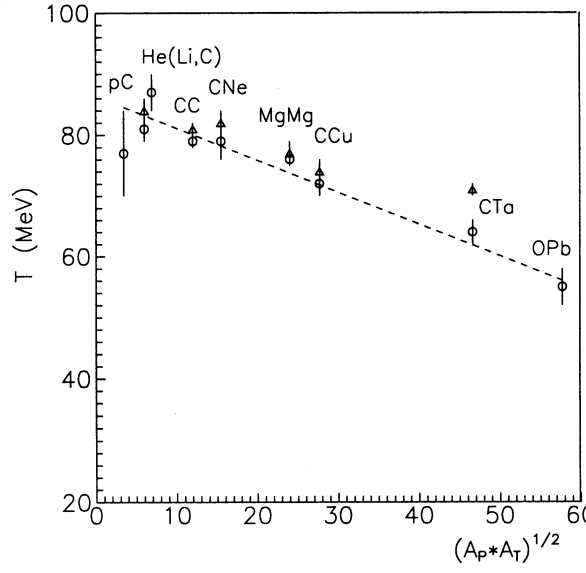

Figure 8. The dependence of the parameter T on $(A_P * A_T)^{1/2}$ for He(Li,C), CNe, MgMg, CCu, OPb [8,9], pC, HeC [10] and our results for semicentral CC and CTa. $\circ$ – experimental data, $\triangle$ – QGSM data. The dashed line is the result of linear approximation of the experimental data.

At the second step 50000 CC and 10000 CTa semicentral collisions have been generated at a fixed impact parameter equal $\langle b \rangle$. The average physical characteristics and analyzing distributions generated for fixed and unfixed impact parameter are coincide within the errors.

The experimental results have been compared with the QGSM generated events for values of $\langle b \rangle$. Figures 1 and 3 present the $\xi^{\pm}$ and $\zeta^{\pm}$ - distributions of π mesons from the QGSM calculations together with the experimental ones for CC and CTa interactions. One can see that the QGSM reproduces experimental distributions well. The QGSM also reproduces the x_F, $cos\theta$ and p_T^2 distributions (Figs. 2, 4 and 5). The QGSM data show similar characteristics in different regions of ζ as experimental ones: sharply anisotropic angular distributions in the region $\zeta^{\pm} < \tilde{\zeta^{\pm}}$ and almost flat distribution in the region $\zeta^{\pm} > \tilde{\zeta^{\pm}}$; the slopes of the p_T^2 – distributions differ greatly in different regions of $\zeta^{\pm}$; the momentum distributions of pions in the laboratory frame in different regions of $\zeta^{\pm}$ have a similarly different shape of spectra as the experimental ones (Fig 6). The momentum distributions of the QGSM data reproduce the corresponding experimental spectra in both regions of $\zeta^{\pm}$. The distributions obtained by the QGSM in the region $\zeta^{\pm} > \tilde{\zeta^{\pm}}$ have been fitted by expressions (8), (9), (10). The results of the fit are given in Table 1 and Figs. 4 and 5. In the region $\zeta^{\pm} < \tilde{\zeta^{\pm}}$, the p_T^2 and $\zeta^{\pm}$ – distributions have been fitted by formulae (12) and (13), respectively. The results of the fit are given in Table 2 and Fig. 5. One can see from Table 1, that the values of T extracted from the experimental and QGSM data agree within the errors for CC and CTa collisions.

Figure 8 shows the dependence of the parameter T from Table 1 on $(A_P * A_T)^{1/2}$, obtained from the experimental and QGSM data together with our previous results [8,9] for He(Li,C), CNe, CCu, MgMg, and OPb interactions obtained on the SKM-200-GIBS set-up and pC and HeC obtained by the Propane Collaboration in [10]. One can see that T decreases linearly with increasing $(A_P * A_T)^{1/2}$, i.e with increasing the number of participating nucleons. A similar behavior is predicted by the QGSM. It is worth to mention that the values of T obtained for semicentral CC and CTa collisions in this paper, agree within the errors with the results for inelastic CC and CTa obtained in [10]. Thus, the values of T seem to depend on the centrality degree very slightly.

5. CONCLUSIONS

The inclusive spectra of pions produced in CC and CTa collisions at a momentum of 4.2 GeV/c per nucleon are analyzed in terms of light front variables ξ and ζ.

1. The results of this paper confirm the conclusions of the previous publications [8,9] that the phase space of secondary π mesons is divided into two regions with respect to maxima value of $\tilde{\zeta^{\pm}}$ ($\tilde{\xi^{\pm}}$).
The angular and momentum distributions of pions in this regions are very different.
2. In one of this kinematical region $\zeta^{\pm} > \tilde{\zeta^{\pm}}$, the $dN/dcos\theta$, dN/dp_T^2, $1/\pi \cdot dN/d\zeta^{\pm}$ distributions are fitted by statistical model predictions. Thus, thermal equilibrium seems to be reached and corresponding temperatures were obtained.
3. The T dependence on $(A_P * A_T)^{1/2}$ is studied. The temperature decreases with increasing $(A_P * A_T)^{1/2}$.
4. The experimental results are compared with the QGSM. The model seems to be in a good agreement with the data.

ACKNOWLEDGEMENTS

The authors express their deep gratitude to N.Amaglobeli for his continuous support. We are very grateful to N.Amelin for providing us with the QGSM code program COLLI. One of the authors (L.Ch.) would like to thank the Board of Directors of the Laboratory of High Energies of JINR for their warm hospitality and also J.Lukstins and O.Rogachevsky for helping during the preparation of the manuscript.

References

[1] A.A. Logunov, M.A. Mestvirishvili and Nguen van Hieu, Phys. Lett. B **25**, 611 (1967).

[2] J. Benecke *et al.*, Phys. Rev. **188**, 2159 (1969).

[3] R. Feynman, Phys. Rev. Lett. **23**, 415 (1969).

[4] V.A. Matveev, R.M. Muradyan and A.N. Tavkhelidze, Lett. Nuovo Cim. **5**, 907 (1972).

[5] A.M. Baldin, Nucl. Phys. A **447**, 203 (1985).

[6] A.A. Baldin, Phys. of Atomic Nuclei **56**, 385 (1993).

[7] A.M. Baldin and L.A. Didenko, Fortschritte der Phys. **38**, 261 (1994).

[8] M. Anikina *et al.*, Nucl. Phys. A **640**, 111 (1998).

[9] M. Anikina *et al.*, Eur. Phys.J. A **7**, 139 (2000).

[10] L. Akhobadze *et al.*, Phys. of At. Nucl. **63**, 1584 (2000).

[11] A. Bondarenko *et al.*, JINR Rapid Communications P1-98-292 (1998).

[12] L. Chkhaidze *et al.*, JINR Preprint E1-2002-255 (Dubna, 2002).

[13] P.A.M. Dirac, Rev. Mod. Phys. **21**, 392 (1949).

[14] N.Ya. Vilenkin and Ya.A. Smorodinsky, Sov. J. of Exp. and Theor. Phys. JETP **47**, 1793 (1964);
V. Garsevanishvili *et al.*, Sov. J. of Theor. and Math. Phys. **7**, 203 (1971).

[15] N.S. Amaglobeli *et al.*, Eur.Phys.J. C **8**, 603 (1999).

[16] V.Garsevanishvili *et al.*, Sov. J. Theor. and Math.Phys. **23**, 310 (1975).

[17] S.J.Chang, R.G.Root and T.M.Yan, Phys.Rev. **D7**, 1133 (1973).

[18] H.Leutwyler, Nucl.Phys. **B76**, 413 (1974).

[19] S.J.Brodsky *et al.*, Particle World **3**, 109 (1993).

[20] K.G.Wilson *et al.*, St.D.Glazek, Phys.Rev. **D49**, 6720 (1994).

[21] B.Desplanques, V.A.Karmanov and J.F.Mathiot, Nucl.Phys. **A589**, 697 (1995);

J.Carbonell *et al.*, Phys.Rep. **300**, 215 (1998).

[22] J. Gunion, SLAC-PUB-2607, September (1980).

[23] N. Amelin *et al.*, Phys. Rev. Lett. **67**, 1523 (1991).

[24] N. Amelin and L. Csernai, In Proc. of the Int. Workshop on Correlations and Multiparticle Production (CAMP), Marburg, Germany, 1990 (World Scientific, Singapore, 1990);
N. Amelin, K. Gudima and V. Toneev, Sov.J. Nucl. Phys. **51**, 327 (1990).

[25] N.Amelin *et al.*, Sov.J. Nucl. Phys. **51**, 535 (1990); **52**, 172 (1990).

[26] N. Amelin, Preprint JINR P2-86-837 (Dubna, 1986).

Received on April 10, 2003.

Чхаидзе Л. В. и др. E1-2003-67
Анализ спектров π^--мезонов в полуцентральных CC- и CTa-соударениях с импульсом 4,2 ГэВ/c на нуклон в переменных светового фронта

Инклюзивные спектры пионов, образованных в CC- и CTa-соударениях с импульсом 4,2 ГэВ/c на нуклон, проанализированы в переменных светового фронта ξ и ζ. Фазовый объем вторичных пионов разделен на две области с существенно различающимися угловыми и импульсными распределениями. В одной из этих областей предположение о термодинамическом равновесии, по-видимому, хорошо согласуется с данными. Изучена зависимость температуры T от $(A_P * A_T)^{1/2}$. T линейно убывает с ростом $(A_P * A_T)^{1/2}$. Результаты сравниваются с предсказанием кварк-глюонной струнной модели. Модель удовлетворительно воспроизводит экспериментальные данные.

Работа выполнена в Лаборатории высоких энергий им. В. И. Векслера и А. М. Балдина ОИЯИ и в Институте физики высоких энергий Тбилисского государственного университета (Грузия).

Препринт Объединенного института ядерных исследований. Дубна, 2003

Chkhaidze L. V. et al. E1-2003-67
The Analysis of π^--Meson Spectra in Semicentral CC and CTa Collisions at a Momentum of 4.2 GeV/c per Nucleon in Terms of Light Front Variables

The inclusive spectra of pions produced in CC and CTa collisions at a momentum of 4.2 GeV/c per nucleon are analyzed in terms of light front variables ξ and ζ. The phase space of the secondary pions is divided into two parts with very different angular and momentum distributions. In one of this part the thermal equilibrium assumption seems to be in good agreement with the data. Corresponding temperatures T are extracted, and their dependence on $(A_P * A_T)^{1/2}$ is studied. T decreases linearly with increasing $(A_P * A_T)^{1/2}$. The results are compared with the predictions of the Quark-Gluon String Model (QGSM). The QGSM satisfactorily reproduces the experimental data.

The investigation has been performed at the Veksler–Baldin Laboratory of High Energies, JINR and at the High Energy Physics Institute, Tbilisi State University (Georgia).

Preprint of the Joint Institute for Nuclear Research. Dubna, 2003

Макет *Т. Е. Попеко*

Подписано в печать 15.05.2003.
Формат 60 × 90/16. Бумага офсетная. Печать офсетная.
Усл. печ. л. 1,43. Уч.-изд. л. 1,97. Тираж 375 экз. Заказ № 53890.

Издательский отдел Объединенного института ядерных исследований
141980, г. Дубна, Московская обл., ул. Жолио-Кюри, 6.
E-mail: publish@pds.jinr.ru
www.jinr.ru/publish/